A Numerical Study for Shape Memory Alloy Bolted Joint for Medical Application

Yanping Wang
College of Medicine
Xi'an International University
Xi'an, People's Republic of China
375031254@qq.com

***Abstract*—Shape memory alloy (SMA) have presented excellent ability for applications in many domains, especially in medical and biomedical applications). Based on the framework of general inelasticity, a 3D super-elastic SMA constitutive model is proposed and implemented successfully into the finite element codes (e.g. ANSYS). The validity of such implementation was finally presented and compared with experimental results of super-elastic NiTi alloy taken from the literature. Finally, this model is used to analyze the stress distribution of a bolted joint for osteopathic medicine.**

Keywords—Shape Memory Alloys, Super-Elasticity, Bolted Joint

I. INTRODUCTION

SMAs are used in many domains including automotive, aerospace, robotic and biomedical and other medical devices and equipments [1]. Some works are carried out on the implementation of constitutive model of SMA into finite element software [2,4]. Auricchio [2] had been implemented a super-elastic constitutive model successfully into the finite element codes, such as ABAQUS and ANSYS. In this work, based on the framework of the generalized plasticity, a temperature-dependent three-dimensional phenomenological constitutive model was developed to describe the thermo-mechanical deformation of super-elastic NiTi alloy. The prediction capability of the proposed model was verified by comparing the simulated results with the experimental ones. Finally, numerical example of finite element calculation is given to verify the validity of the implementation, and applied to the analysis of the stress distribution of a bolted joint.

II. CONSTITUTIVE MODEL

Generalized plasticity is firstly employed by Saint-Sulpice [5] to describe the thermo-mechanical responses of shape memory alloys. It is a local internal variable theory of rate-independent inelastic behavior which is based primarily on the loading-unloading irreversibility. The general mathematical foundation provides the theory the ability to deal with the non-standard cases such as non-connected elastic domains. With infinitesimal strain assumption, the additively decomposition of the total strain $\tilde{\boldsymbol{\varepsilon}}$ into an elastic strain $\tilde{\boldsymbol{\varepsilon}}_{\mathrm{e}}$ and an inelastic strain $\tilde{\boldsymbol{\varepsilon}}_{\mathrm{in}}$ yields:

$$\tilde{\boldsymbol{\varepsilon}} = \tilde{\boldsymbol{\varepsilon}}_{\mathrm{e}} + \tilde{\boldsymbol{\varepsilon}}_{\mathrm{in}} \tag{1}$$

Based on the assumption of small deformation, the total inelastic strain $\tilde{\boldsymbol{\varepsilon}}_{\mathrm{in}}$ is the stress-induced martensitic transformation $\tilde{\boldsymbol{\varepsilon}}_{\mathrm{t}}$. As a result, the total strain expression is:

$$\tilde{\boldsymbol{\varepsilon}} = \tilde{\boldsymbol{\varepsilon}}_{\mathrm{e}} + \tilde{\boldsymbol{\varepsilon}}_{\mathrm{in}} = \tilde{\boldsymbol{\varepsilon}}_{\mathrm{e}} + \tilde{\boldsymbol{\varepsilon}}_{\mathrm{t}} \tag{2}$$

After discretizing of the equations, the expressions are as follows:

$$\Delta\tilde{\boldsymbol{\varepsilon}}_{\mathrm{in}} = \Delta\tilde{\boldsymbol{\varepsilon}}_{\mathrm{t}} \tag{3}$$

$$\Delta\tilde{\boldsymbol{\varepsilon}}_{\mathrm{e}} = \Delta\tilde{\boldsymbol{\varepsilon}} - \Delta\tilde{\boldsymbol{\varepsilon}}_{\mathrm{t}} \tag{4}$$

The stress-induced martensitic transformation and its reverse transformation which can be defined by the volume fraction of martensite as the internal variable $\tilde{\xi}$. The elastic stress-strain relation can be then expressed as:

  DOI: 10.25236/iccpb.2018.014

$$\tilde{\boldsymbol{\sigma}} = \tilde{\boldsymbol{\sigma}}^{*} - \tilde{\mathbf{D}}^{\mathrm{e}}\left(\tilde{\xi}\right) : \Delta\tilde{\boldsymbol{\varepsilon}}_{\mathrm{in}} \tag{5}$$

where $\tilde{\mathbf{D}}^{\mathrm{e}}(\tilde{\xi})$ is the equivalent elastic tensor [6,8], and $\tilde{\mathbf{D}}^{\mathrm{e}}(\tilde{\xi}) = [(1-\tilde{\xi})\tilde{\mathbf{D}}_A^{-1} + \tilde{\xi}\tilde{\mathbf{D}}_M^{-1}]^{-1}$, where $\tilde{\mathbf{D}}_A$ and $\tilde{\mathbf{D}}_M$ are the elastic tensor of austenite and martensite, respectively. Considering the deviatoric stress of the above equation, it can be gotten $\tilde{\mathbf{D}}^{\mathrm{e}} : \Delta\tilde{\boldsymbol{\varepsilon}}_{\mathrm{in}} = 2\tilde{G}\Delta\tilde{\boldsymbol{\varepsilon}}_{\mathrm{in}}$, and:

$$\tilde{\mathbf{s}} = \tilde{\mathbf{s}}^{*} - 2\tilde{G}\Delta\tilde{\boldsymbol{\varepsilon}}_{\mathrm{in}} \tag{6}$$

where $\tilde{G}$ is the shear elastic modulus, and $\tilde{\mathbf{s}}^{*}$ is the deviatoric stress of $\tilde{\boldsymbol{\sigma}}^{*}$.

As mentioned in the references [9, 11], some phase transformations are pressure-dependent. To model such an effect, the Von-Mises-typed transformation surfaces are introduced:

$$\tilde{F}(\tilde{\boldsymbol{\sigma}}, q) = \tilde{\boldsymbol{\sigma}}_{\mathrm{eq}} - \tilde{\boldsymbol{\sigma}}_{\mathrm{y}}(q) = 0 \tag{7}$$

where $\tilde{\boldsymbol{\sigma}}_{\mathrm{eq}} = \left[\frac{3}{2}\tilde{\mathbf{s}} : \tilde{\mathbf{s}}\right]^{\frac{1}{2}}$ is the von Mises equivalent stress. The phase transformation to describe the forward transformation and its reverse transformation are introduced as follows:

$$\tilde{F}_{\mathrm{AM}}(\tilde{\boldsymbol{\sigma}}, q) = \tilde{\boldsymbol{\sigma}}_{\mathrm{eq}} - \sigma_{s,T}^{\mathrm{AM}}(\tilde{\xi}) = 0\,, \text{ forward transformation} \tag{8a}$$

$$\tilde{F}_{\mathrm{MA}}(\tilde{\boldsymbol{\sigma}}, q) = \tilde{\boldsymbol{\sigma}}_{\mathrm{eq}} - \sigma_{s,T}^{\mathrm{MA}}(\tilde{\xi}) = 0\,, \text{ reverse transformation} \tag{8b}$$

where, $\sigma_{s,T}^{\mathrm{AM}}$ and $\sigma_{s,T}^{\mathrm{MA}}$ are the start stresses of the forward transformation and the reverse transformation, respectively.

In this paper, the reversible martensite volume fraction $\tilde{\xi}$ can be related to the transformation strain $\tilde{\varepsilon}_{\mathrm{t}}$ by the following formula:

$$\tilde{\xi} = \tilde{\varepsilon}_{\mathrm{t}} / \varepsilon_{\mathrm{L}} \tag{9}$$

where, ε_{L} is the maximum phase transformation strain under uniaxial tension, which can be determined by the experimental test under loading and unloading. Similar to the classical plasticity, the transformation strain rates obey the normality rule, i.e., they are normal to the transformation surface in the stress space as

$$\Delta\tilde{\boldsymbol{\varepsilon}}_{\mathrm{t}}^{\mathrm{AM}} = \sqrt{\frac{3}{2}}\varepsilon_{\mathrm{L}}\Delta\tilde{\xi}\mathbf{n}_{\mathrm{AM}}, \Delta\dot{\tilde{\xi}} > 0\,, \text{ forward phase transformation} \tag{10a}$$

$$\Delta\tilde{\boldsymbol{\varepsilon}}_{\mathrm{t}}^{\mathrm{MA}} = \sqrt{\frac{3}{2}}\varepsilon_{\mathrm{L}}\Delta\tilde{\xi}\mathbf{n}_{\mathrm{MA}}, \Delta\dot{\tilde{\xi}} < 0\,, \text{ reverse phase transformation} \tag{10b}$$

with

$$\mathbf{n}_{\mathrm{AM}} = \frac{\partial\tilde{F}_{\mathrm{AM}}(\tilde{\boldsymbol{\sigma}}, \tilde{\xi})}{\partial\tilde{\boldsymbol{\sigma}}} = \sqrt{\frac{3}{2}}\frac{\tilde{\mathbf{s}}}{\tilde{\boldsymbol{\sigma}}_{\mathrm{eq}}} \tag{11a}$$

$$\mathbf{n}_{\mathrm{MA}} = \frac{\partial \tilde{F}_{\mathrm{MA}}(\tilde{\boldsymbol{\sigma}}, \tilde{\xi})}{\partial \tilde{\boldsymbol{\sigma}}} = \sqrt{\frac{3}{2}} \frac{\tilde{\mathbf{s}}}{\tilde{\boldsymbol{\sigma}}_{\mathrm{eq}}} \tag{11b}$$

In this paper, the phase transformation, austenite yield and martensite yield behavior under different temperature are considered in the process of implicit stress integral solution.

In general, it is assumed that the stress-induced martensitic transformation, and there is no interaction between them. The isotropic elastic-plastic constitutive model with implicit stress integration method is extended to that method of the constitutive modeling of SMA. According to the above assumptions, Equation (6) can be further expressed as follows for the implicit stress integration process of the phase change behavior:

$$\tilde{\mathbf{s}} = \tilde{\mathbf{s}}^{*} - 2\tilde{G}\Delta\tilde{\boldsymbol{\varepsilon}}_{\mathrm{t}} \tag{12}$$

By Equations (10a-b), it can be obtained:

$$\Delta\tilde{\boldsymbol{\varepsilon}}_{\mathrm{t}}^{\mathrm{AM}} = \sqrt{\frac{3}{2}}\varepsilon_{\mathrm{L}}\Delta\tilde{\xi}\mathbf{n}_{\mathrm{AM}}, \Delta\dot{\tilde{\xi}} > 0 \text{ , forward phase transformation} \tag{13a}$$

$$\Delta\tilde{\boldsymbol{\varepsilon}}_{\mathrm{t}}^{\mathrm{MA}} = \sqrt{\frac{3}{2}}\varepsilon_{\mathrm{L}}\Delta\tilde{\xi}\mathbf{n}_{\mathrm{MA}}, \Delta\dot{\tilde{\xi}} < 0 \text{ , reverse phase transformation} \tag{13b}$$

III. Verification of Proposed Model

Before you begin to format your paper, first write and save the content as a separate text file. Complete all content and organizational editing before formatting. Please note sections A-D below for more information on proofreading, spelling and grammar.

Keep your text and graphic files separate until after the text has been formatted and styled. Do not use hard tabs, and limit use of hard returns to only one return at the end of a paragraph. Do not add any kind of pagination anywhere in the paper. Do not number text heads-the template will do that for you.

The results of the phase transformation simulations by the proposed model are compared with the experimental data by Kang [12]. To verify the proposed model, the super-elastic stress-strain curves at different temperatures are simulated using the parameters listed as follows to identify the parameters:

$E_{\mathrm{A}}^{T_0}$ =41.0GPa, $E_{\mathrm{M}}^{T_0}$ =37.0GPa; $\nu_A = \nu_M$ =0.33; C_{AM} =8.0MPa/K, C_{MA} =8.8MPa/K; k =0.16; $\sigma_{s,T0}^{AM}$ =353.0MPa, $\sigma_{f,T0}^{AM}$ =381.0MPa, $\sigma_{s,T0}^{MA}$ =141.0MPa, $\sigma_{f,T0}^{MA}$ =122.0MPa; ε_L =0.035; T_0 =295K; $h_{\mathrm{M}}^{\mathrm{p}}$ = 6.7GPa.

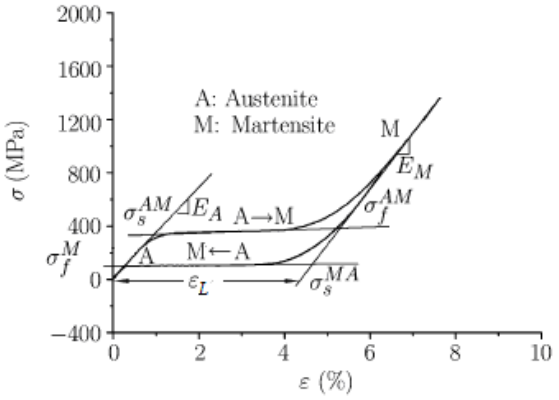

Fig. 1. SMA phase transformation and plasticity behavior diagram

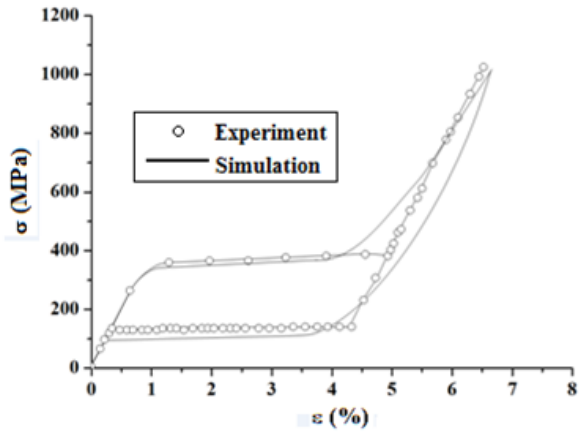

Fig. 2. Uniaxial tension and unloading of NiTi shape memory alloy with phase transformation

The uniaxial tension and unloading case of the material is calculated based on the proposed model. The simulation results are shown in Figure 2. It can be seen from Figure 2 that the stress-induced martensitic transformation occurs. As the load is lower than the phase transformation finish stress $\sigma_{f,T}^{MA}$, the austenite will take place elastic unloading as following. That elastic unloading curve is coincident with the initial elastic loading one. It can be seen from Figure 2 that the response peak stress is about 1000MPa, and the martensite can still be completely transformed into austenite when unloading. The simulated results show good agreement with the experimental ones. The results show that the proposed constitutive model can predict the thermodynamic behavior in the super-elastic NiTi alloy. It can be predicted that the model can also give a reasonable prediction results for other working conditions and other experimental results in the temperature range.

IV. Finite Element Analyses for the SMA Bolted Joint

In this section, the proposed constitutive model is used to be carried out to analyze the stress distribution of a bolted joint. The mesh model is in Figure 3. Because the SMA bolted joint structure is a spatial axisymmetric structure, only the section map is selected to establish the finite element model in this research to simulate the stress distribution of the bolted joint under the axial bolted preload. The type of element is set four-noded plane element 182 with the isotropic character. The Young's modulus of members is set as 209GPa, and the Poisson's ratio is 0.3. The contact surface element CONTA172 and the target surface element TARGE169 are used to generate contact pairs of the finite element model. The bolt pretightening element Prets179 is used to produce the preloading force of the bolt.

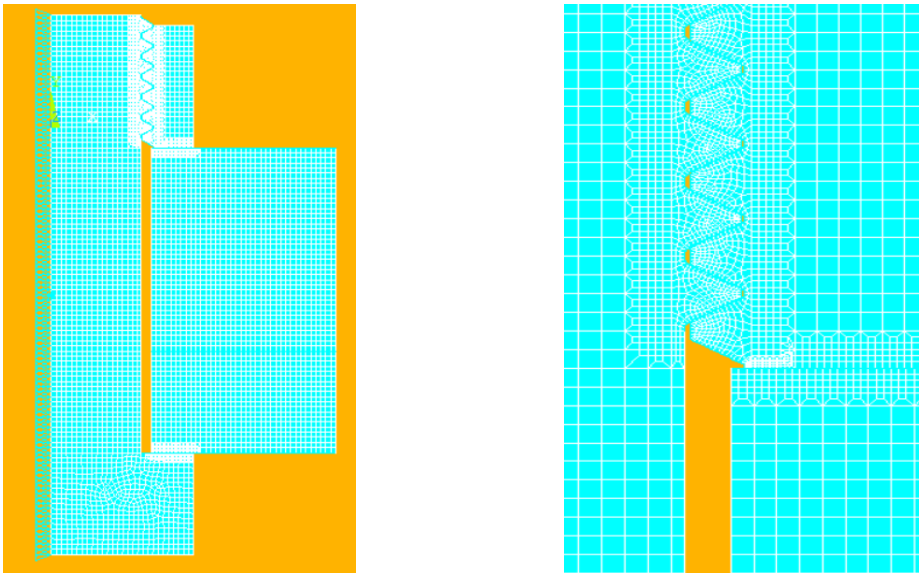

(a) (b)

Fig. 3. Two-dimensional mesh model of bolted joint: (a) Overall model, (b) Local refined model

In this study, the finite element model of bolt is in first preloaded and unloaded. The equivalent stress cloud chart of the finite element model after calculation is observed, as shown in Figures 4 (a) and (b). The two stress cloud maps correspond to the A and B points of the stress-strain curve of the node 1, as shown in Figure 5 (a). The A point indicates the end time of martensitic transformation, but no plastic deformation occurs. When the load continues to reach the B point, it indicates that the plastic deformation has occurred and the peak stress is 1746MPa. Because the peak stress is higher than the plastic yield stress of martensite, the plastic deformation of superelastic NiTi alloy continues to occur after the martensite elastic deformation, and

the deformation goes through three stages. Due to the plastic deformation of martensite, some residual deformation will be produced after unloading. This part of the deformation can not be recovered after unloading, which leads to the lose of the superelastic part of the NiTi alloy. The stress strain curve of node 2 shown in Figure 5 (b) shows that the stress concentration of bolt screw thread is more relieved than the stress concentration in the load part of the nut, which is far from the martensitic plastic yield point. However, it can be found an obvious superelasticity. When the bolt preload is unloaded, the stress returns to the initial zero point. From the above discussions, the results of the ANSYS simulation based on the proposed model are in good agreement with the the uniaxial tensile test results of SMA, which also shows that the finite element implementation of the constitutive model is valid.

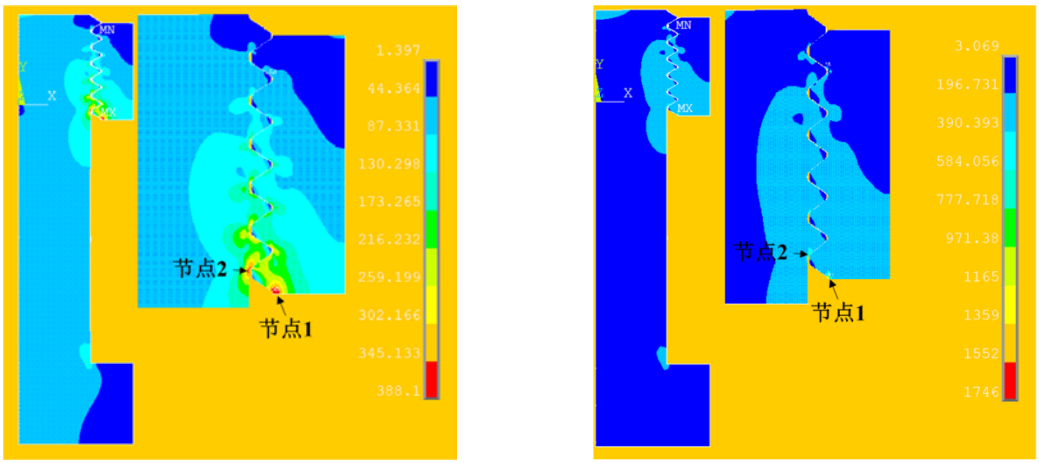

(a) (b)

Fig. 4. (a) Equivalent stress cloud map at the end of martensitic phase transition, (b) Equivalent stress cloud map at martensitic plastic yield moment

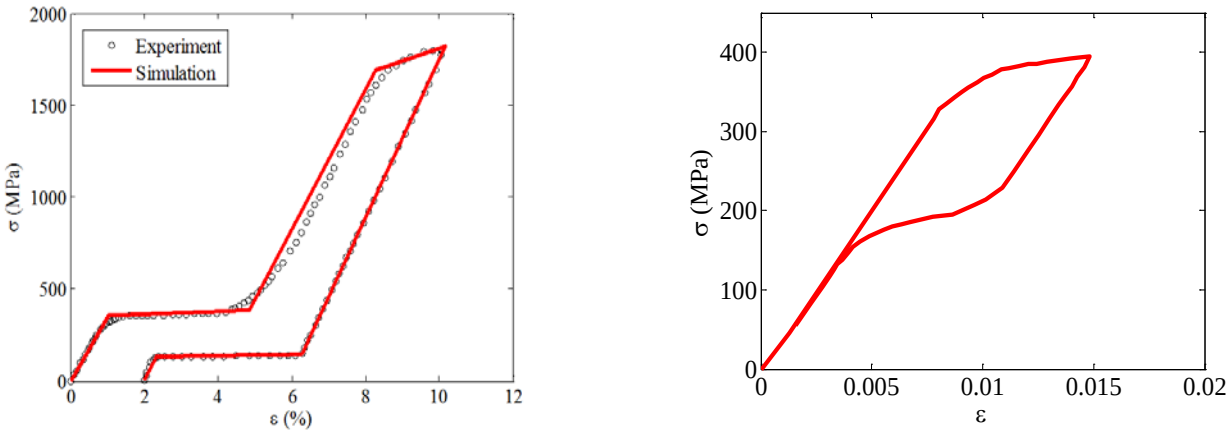

(a) (b)

Fig. 5. (a) Stress-strain curve of node 1 at different times, (b) Stress-strain curve of node 2 at different times

V. Conclusions

A SMA phenomenological constitutive model with implementation into the finite element code ANSYS is proposed in the general inelastic framework. The numerical results show the good simulation results compared with the experimental ones. Finally, the numerical analyses for a SMA bolted joint present the reasonable stress distribution and stress-strain curve of different node at different times.

Acknowledgment

We would like to thank for the financial support of this work by the National Natural Science Foundation of China (NSFC) under Grant Number 51775406, the Fundamental Research Funds for the Central Universities (Grant No. JB180412), the Natural Science Foundation of Shanxi Province of China (Grant No. 2017JM5035).

References

[1] J.M. Jani, M. Leary, A. Subic, “A review of shape memory alloy research, applications and opportunities', Mater. Design., vol. 56, pp.1078–1113, 2014.

[2] F. Auricchio, R.L. aylor, “Shape-memory alloy modeling and numerical simulations of the finite-strain superelastic behavior,” Comput. Method Appl. Mech. Eng., vol.143, pp.175-194, 1997.

[3] F. Auricchio, “A robust integration algorithm for a finite strain shape memory alloy superelastic model,” Int. J. Plasticity, vol. 17, pp. 971-990, 2001.

[4] N. Rebelo, M. Hsu, H. Foadian, “Simulation of super-elastic alloys behavior with abaqus,” Proc. Int. Conf. on Shape memory and Super-elastic Technologies. SMST, Pacific Grove (USA, 2001), pp. 457-469, 2000.

[5] L. Saint-Sulpice, S.A. Chirani, S. Calloch, “A 3D superelastic model for shape memory alloys taking into account progressive strain under cyclic loadings,” Mech. Mater., vol. 41, pp.12-26, 2009.

[6] Y. Ivshin, T. Pence, “A thermomechanical model for a one variant shape memory material,” J. Intel Mat. Syst Str., vol. 5, pp.455-473, 1994.

[7] F. Auricchio, S. Marfia, E. Sacco, “Modelling of SMA materials: Training and two way memory effects,” Comp. Struct., vol. 81, pp.2301-2317, 2003.

[8] W. Zaki, Z. Moumni, “A 3-D model of the cyclic thermomechanical behavior of shape memory alloys,” J Mech. Phys. Solids., vol. 55, pp.2427-2454, 2007.

[9] C. Liang, C. Rogers, “One-dimensional thermomechanical constitutive relations for shape memory materials,” J. Intel Mat. Syst Str., vol. 1, pp.207-234, 1990.

[10] F. Auricchio, E. Sacco, “A one-dimensional model for superelastic shape memory alloys with diffeent elastic properties between austenite and martensite,” Int. J Nonlin. Mech., vol. 32, pp.1101-1114, 1997.

[11] X.J. Jiang, B.T. Li, “Finite element analysis of a superelastic shape memory alloy considering the effect of plasticity,” J. Theor. App. Mech., vol. 55(4), pp.1355-1368, 2017.

[12] G.Z. Kang, Q.H. Kan, L.M. Qian, “Ratchetting deformation of super-elastic and shape-memory NiTi alloys,” Mech. Mater., vol. 41, pp.139-153, 2009.